Agri. & Biosys. Eng. Vol. 7(1):1-7(2006)

Finite Element Prediction of Temperature Distribution in a Solar Grain Dryer

H. Uluko, J. T. Mailutha, C. L. Kanali, D. Shitanda, H. Murase

Abstract: A need exists to monitor and control the localized high temperatures often experienced in solar grain dryers, which result in grain cracking, reduced germination and loss of cooking quality. A verified finite element model would be a useful to monitor and control the drying process. This study examined the feasibility of the finite element method (FEM) to predict temperature distribution in solar grain dryers. To achieve this, an indirect solar grain dryer system was developed. It consisted of a solar collector, plenum and drying chambers, and an electric fan. The system was used to acquire the necessary input and output data for the finite element model. The input data comprised ambient and plenum chamber temperatures, prevailing wind velocities, thermal conductivities of air, grain and dryer wall, and node locations in the xy-plane. The outputs were temperature at the different nodes, and these were compared with measured values. The ±5% residual error interval employed in the analysis yielded an overall prediction performance level of 83.3% for temperature distribution in the dryer. Satisfactory prediction levels were also attained for the lateral (61.5-96.2%) and vertical (73.1-92.3%) directions of grain drying. These results demonstrate that it is feasible to use a two-dimensional (2-D) finite element model to predict temperature distribution in a grain solar dryer. Consequently, the method offers considerable advantage over experimental approaches as it reduces time requirements and the need for expensive measuring equipment, and it also yields relatively accurate results.

Keywords: 2-D FEM, Solar Dryer, Temperature Distribution, Postharvest Grain Losses

Introduction

Developing countries, particularly those in the sub-Saharan Africa, suffer heavy postharvest grain losses. Direct grain losses are mainly caused by rodents, birds, spillage and contamination, and are often as high as 10–25% (Kristoferson and Bokalders, 1991; Nindo, 1995). In Kenya, for example, postharvest cereal grain losses range from 18–25% (Nindo, 1995). This high level of grain loss is of critical economic importance to countries such as Kenya that largely rely on agricultural produce for its foreign exchange.

The high moisture content at which grains are harvested necessitates the use of dryers to remove excess moisture in order to minimize losses and quality deterioration. Commercial dryers have extensively been used to dry grain (Kristoferson and Bokalders, 1991). In most current commercial crop dryers; heat for the drying process is generated by combustion of oil, gas, wood or by electrical means. Such drying methods are unaffordable to small-scale farmers in rural areas as the fuels and the dryers are costly and hence are not readily available to them. Furthermore, the exhaust gases emitted from combustion of most fuels are often dirty and may be toxic. A heat exchanger, which is also expensive, is required in order to avoid contamination of the material being dried.

Solar grain dryers have previously been used with success for drying grain with considerable reduction in grain losses as opposed to floor or field sun drying (Bonazzi *et al.*, 1994). They offer numerous advantages such as protection of drying material from contamination, quick drying (1–2 days) and superior milling and germination qualities. However, at times high temperatures, which may be 30°C above ambient temperature, are induced in the dryers (Saleh and Sarker, 2002). High dryer temperatures result in grain cracking and reduced quality (Bonazzi *et al.*, 1994). There is therefore need to determine temperature distribution in grain dryers in order to monitor and control the drying process, for safe drying and product quality maintenance. This can be achieved either by physical

The authors are **H. Uluko, D. Shitanda**, Bunda College of Agriculture, Agricultural Engineering Department, P.O. Box 219, Lilongwe, Malawi; **J. T. Mailutha, C. L. Kanali**, Biomechanical and Environmental Engineering Department, Jomo Kenyatta University of Agriculture and Technology, P.O. Box 62000-00200, Nairobi, Kenya; **H. Murase**, Laboratory of Bioinstrumentation Control and Systems Engineering, College of Agriculture, Osaka Prefecture University. **Corresponding author:** H. Murase Laboratory of Bioinstrumentation Control and Systems Engineering, College of Agriculture, Osaka Prefecture University, 1-1 Gakuencho, Sakai, Osaka 599-8531, Japan; e-mail: hmurase@bics.envi.osakafu-u.ac.jp

measurements of temperature or by the use of models for prediction. Conducting experiments to study the temperature distributions in dryers is an expensive and time-consuming process (Jia *et al.*, 2000). The use of prediction techniques may be suitable alternatives to experimental methods. The prediction models can handle diverse and complex problems often found in biological products (Jia and Cao, 1998).

During solar drying, boundary conditions change with ambient conditions; hence it is difficult to develop an analytical solution for heat transfer when predicting temperature distribution (Basunia *et al.*, 1996). As an alternative to this, numerical methods are applied, which include Finite Difference Method (FDM), Finite Volume Method (FVM), Boundary Element Method (BEM), and Finite Element Method (FEM). FDM is not completely satisfactory for the engineering analysis of biological materials such as grains that have large variations in material properties (Jia *et al.*, 2000; Basunia *et al.*, 1996). It is also cumbersome when the geometries of the systems (e.g., dryers) being considered have curved boundaries, which makes it difficult to develop a computer program for the method (Segerlind, 1984). FDM and FVM are only effective on rectangular domains in higher dimensions, which make their scope severely limited. BEM has experienced stunted commercial development because of its computationally intensive solvers, which require high computer memory.

The FEM has gained reputation as an alternative to analytical or statistical models in solving engineering problems often found in non-linear biological systems. For example, FEM has been used to predict transient temperature distribution in a grain storage bin (Basunia *et al.*, 1996; Jia *et al.*, 2000), and analysis of temperature distribution in the interior of plant culture vessel (Suroso *et al.*, 1995). In spite of these, it has not been used in the prediction of temperature distribution in solar grain dryers. Therefore, this study aimed at using a verified finite element model for prediction of temperature distribution in solar grain dryers.

Materials and Methods

1. Equipment Development

The study was conducted at Jomo Kenyatta University of Agriculture and Technology (JKUAT) in September 2003. JKUAT is located in Juja (1° 05'S latitude and 37° 00'E longitude), which is near Nairobi, the capital city of Kenya. The solar grain dryer developed in this study (Figure 1) consisted of a centrifugal fan for blowing air into the system, air ducts, a flat plate solar collector, and plenum and drying chambers. The solar collector was tilted at an

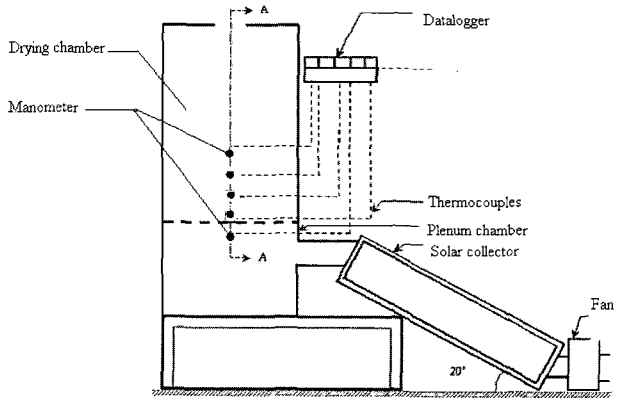

Fig. 1 Schematic diagram of the solar dryer and data acquisition system.

angle of 20° in order to trap maximum insolation. The dimensions of the collector were 1200x600x160 mm (length, width and height). It was made from chipboard with a thickness of 13 mm, which served as an insulating material. The inside was painted black to enhance the trapping of solar radiation. A 4 mm thick transparent glass was used as cover for the solar collector. The solar collector was connected to the centrifugal fan and the plenum chamber by air ducts. The air ducts were made from polyvinyl chloride pipe of diameter 100 mm. The heated air from the solar collector was mixed in the plenum chamber measuring 420x420x250 mm, so as to attain uniform air temperature prior to entry into the drying chamber, measuring 420x 420x450 mm. Five holes (four on the drying chamber and one on the plenum chamber) measuring 5 mm in diameter, through which T-type thermocouples (for registering ambient, plenum and grain temperatures) were inserted, were drilled along the central line of one side of the dryer. The holes were spaced at 40 mm interval (Figure 2a) with the lower hole on the drying chamber located at 15 mm from the bottom.

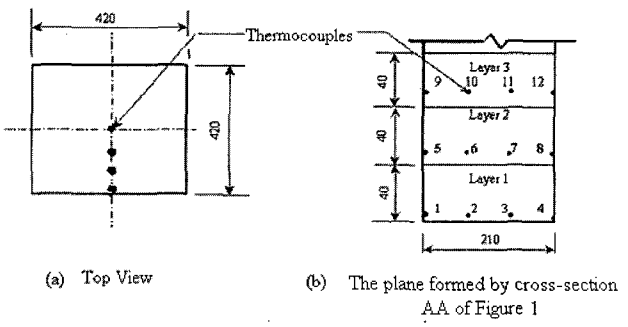

Fig. 2 Location of thermocouples in the drying chamber; measurements are in millimeters

2. Data Acquisition and Analysis

The equipment shown in Figure 1 was used to acquire the necessary data. Basmati-378 rice, a dominant rice cultivar grown in Mwea Irrigation Scheme (Kenya), was used in the study. The paddy rice was cleaned by removing broken, weathered and immature particles and foreign materials. The rice was rewetted at room temperature for 24 hours (ASAE standards, 1997). It was then loaded in the dryer to a depth of 120 mm without packing, and then leveled manually. Airflow of 2 m/s was used to drive heated air through the drying system. The data was automatically recorded by a data logger. An anemometer and a humidity sensor were employed to record the ambient wind velocity and relative humidity, and the relative humidity in the plenum and drying chambers at 30-minute intervals for the whole period of drying. Hourly solar insolation data was obtained from a pyrometer at the JKUAT meteorological station. A water manometer was used to measure pressure drop across the grain bed at 2-hour intervals.

The initial moisture content of the grain was about 49% (d.b.). The temperature of air in the plenum chamber and the pressure drop across the grain bed did not vary significantly in the course of drying. On average, the plenum temperature and the pressure drop were 45.6°C and 75 cm of water, respectively. The mean ambient temperature and plenum chamber relative humidity were 26.5°C and 35%, respectively. Solar radiation varied between 200 and 600 W/m^2. Data acquisition involved recording grain temperature values at intervals of 30 minutes for 12.5 hours. The first set of data (corresponding to time zero hours) was recorded after 30 minutes of airflow through the solar dryer to allow conditions in the system stabilize.

The data collected was used by a simulated two-dimensional (2-D) grain dryer model to predict temperature distribution in the dryer. The model was defined by an area of discrete grid points ($x_i y_j$), as shown in Figure 3, on which m vertical lines and n horizontal lines were distributed. The grid was identical to the plane formed by cross section AA (Figure 2b). Since the dryer studied was symmetrical about the central plane along cross section AA, only a half of the total region was meshed and considered for the analysis. The discrete points were located at the intersections of the horizontal and vertical lines and their coordinates were established from equations (1) and (2), where W and H are the width and height of the grain drying chamber, respectively. In this study, m=5, n=12, W=210 mm, and H=450 mm.

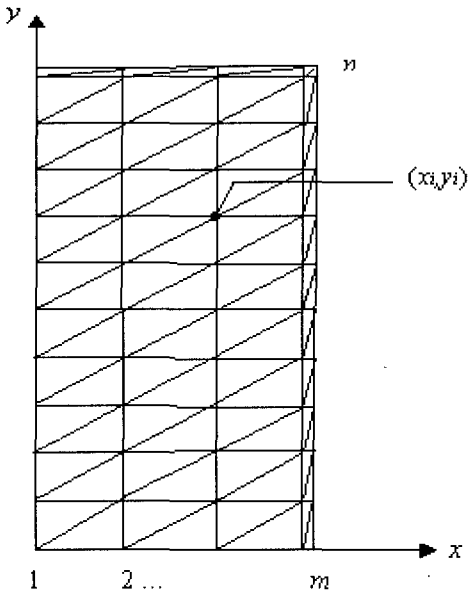

Fig. 3 The finite element discretization of the grain-drying chamber.

$$x_i = (i-1)\frac{W}{(m-1)}\Big|_{i=1\text{ to }m} \quad (1)$$

$$y_i = (i-1)\frac{H}{(n-1)}\Big|_{i=1\text{ to }n} \quad (2)$$

The mesh of triangular elements consisted of 60 nodes (Figure 3). However, the nodes of interest were Nodes 1-12 (Figure 2b). Nodes 1-12 were on the boundary and within the 120 mm grain layer while the rest represented the remaining portion of the dryer above the 120 mm grain layer. Triangular elements were chosen because they are widely used in structural, heat and mass diffusion problems (Suroso *et al.*, 1995; Jia *et al.*, 2000). Triangular elements are simple to use hence more elements can be used in the region that defines the problem of interest and this yields relatively accurate results (Baker and Pepper, 1991). The simulated dryer model was linked to a modified FEM program coded FINEL (Suroso *et al.*, 1995). The modification involved changing the equations from axisymmetrical to plane coordinates problem.

The modified finite element model was developed from the 2-D partial differential equation describing the steady state heat conduction transfer through the grain, which is given by (Segerlind, 1984; Holman, 1992) :

$$k\frac{\partial^2 T}{\partial x^2} + k\frac{\partial^2 T}{\partial y^2} + q_r = 0 \quad (3)$$

where : k is the thermal conductivity of the grain in W/m K, q_r is the rate of heat generated in the dryer in W/m^3, T is the grain temperature in K, and x and y are the plane coordinates. The bottom layer of the grain in the drying chamber is in contact with plenum temperature, in which case, boundary condition s_1 exists and is given as shown in equation (2), where T_p is the plenum temperature.

$$T = T_p \tag{4}$$

The drying chamber wall is exposed to wind velocity, v, and ambient temperature, T_a, which result in the boundary condition s_2 existing around the wall, and is given as in equation (5). In this equation, **n** is normal vector and h is the convective heat transfer coefficient in W/m^2 K.

$$k\nabla T.\mathbf{n} + h_{s_2}(T - T_a) = 0 \tag{5}$$

Equations used for calculating convective heat transfer coefficient are detailed in Holman (1992). The dryer wall is also affected by heat fluxes, q_n in W/m^2 presented by equation (6) and boundary condition s_3 exist.

$$k\nabla T.\mathbf{n} + q_n = 0 \tag{6}$$

The union of s_1, s_2, and s_3 forms the complete boundary on the surface, s, of the problem domain. Equation (3) and boundary conditions, equations (4)-(6), can be written in matrices form as (Baker and Pepper, 1991):

$$[K]\{T\} - \{b\} = 0 \tag{7}$$

where [K] is the global stiffness (conductivity) matrix created from the stiffness matrix of each element. The variables {T} and {b} are the temperature vector and the thermal force (load) vector, respectively. The full derivation of equation (7) can be found elsewhere (Baker and Pepper, 1991). Equation (7) is solved by the Gauss elimination procedure and a simulation program using the finite element method based on the above analyses was developed to predict temperature distribution of grain in the solar grain dryer.

Input data to the finite element model were wind velocity, ambient and plenum chamber temperatures, nodal locations, grain depth, and thermal conductivities of grain, drying chamber wall and air (Table 1). The outputs were temperatures at the different nodes, and these were compared with actual values. The comparison involved determining the absolute residual errors (ε) as shown in equation (8), where ψ_p and ψ_m are the predicted and actual values,

Table 1 Thermal and physical properties of the experimental solar dryer and materials used

Materials	*Density* (kg/m^3)	*Thermal conductivity* ($W/m\ K$)	*Specific heat* ($J/kg\ K$)
Rice	636	0.14	2110
Plywood	545	0.16	1215
Air	-	0.03	-

Source : Horacek, 2003; Jia *et al.*, 2000; Holman, 1992

respectively.

$$\varepsilon(\%) = \left| \frac{(\psi_p - \psi_m)}{\psi_m} \times 100 \right| \tag{8}$$

Thereafter, based on a 5% residual error interval, the prediction performance (η) of the model was determined by equation (9), where N_c and N_t represent the number of data within the interval and trial data, respectively. Linear regression analysis (MS Excel 2000^{TM}) was also conducted to relate the predicted and measured nodal temperature data.

$$\eta(\%) = 100 \times \frac{N_c}{N_t} \tag{9}$$

Results and Discussion

Table 2 shows the data acquired for grain temperature distribution during the drying period for the bottom (Nodes 1-4), middle (Nodes 5-8) and top (Nodes 9-12) layers. The node numbering employed is related to the location of the thermocouples as shown in Figure 2(b). Nodes 1, 5 and 9, and 4, 8 and 12 are at the center and on the sides of the drying chamber, respectively. From the table, it is seen that a temperature gradient exists across the drying chamber with the inside being hotter than the sides, as also observed by Oosthuizen (1987) and Jia *et al.* (2000) for temperature in natural convection dryers. Since the ambient air temperature was lower than the plenum temperature (Figure 4), this resulted in high heat losses on the sides of the drying chamber. The table further shows that the percentage of data for the bottom, middle and top layers with a defined temperature gradient existing across the dryer were 46.2, 65.4 and 73.1%, respectively. No reasonable explanation could be attributed to this observation. The mean (y-direction) values indicate that there was a decrease in temperature from the bottom to the top layer as expected due to heat

Table 2 Temperature (°C) distribution in the rice layer during drying

Drying time (Hours)	Bottom layer				Middle layer				Top layer			
	Node number											
	1	2	3	4	5	6	7	8	9	10	11	12
0.0	34.1	33.0	32.4	26.5	31.9	31.8	29.4	24.6	31.8	29.8	31.5	25.6
0.5	30.2	29.8	29.7	27.9	28.1	27.0	29.0	25.1	29.7	29.7	27.2	26.3
1.0	31.0	31.8	30.4	26.0	32.0	29.9	29.9	24.7	32.2	32.2	31.1	26.3
1.5	29.0	27.0	29.7	26.1	29.8	29.0	28.4	24.9	29.1	28.9	29.2	25.0
2.0	29.4	28.7	28.4	26.4	29.4	28.7	28.1	24.0	29.5	29.1	28.9	24.4
2.5	29.1	29.0	29.6	24.9	28.7	28.0	27.0	24.4	29.4	28.4	28.7	25.1
3.0	30.2	30.4	30.1	26.4	29.9	29.4	27.7	25.8	32.0	29.8	29.7	25.9
3.5	29.8	30.1	30.1	26.7	30.4	29.9	28.7	25.0	29.8	29.7	30.1	25.4
4.0	29.9	30.5	29.9	27.7	31.8	29.4	29.0	26.1	31.6	33.0	30.6	26.1
4.5	33.7	32.7	31.9	30.0	34.9	32.0	31.5	29.8	34.9	33.7	31.3	31.1
5.0	33.0	34.9	34.6	32.1	35.4	34.2	33.8	31.2	34.9	34.5	35.6	29.3
5.5	34.7	35.6	34.5	29.9	32.9	34.6	33.0	29.5	33.1	32.4	32.7	28.2
6.0	32.9	32.9	32.6	29.1	33.1	30.9	30.2	27.0	32.9	31.1	34.4	27.9
6.5	36.0	34.0	31.9	26.9	31.4	32.0	27.8	26.7	30.8	30.7	25.8	26.2
7.0	30.5	30.5	27.9	27.1	30.1	28.0	28.0	25.4	30.3	29.8	26.8	26.4
7.5	32.5	32.4	31.2	26.5	30.2	32.0	30.1	24.9	30.5	30.4	30.0	25.3
8.0	30.5	29.0	30.1	25.0	29.7	27.5	29.4	27.4	30.2	29.0	29.9	25.2
8.5	30.4	29.8	28.1	26.4	29.5	27.0	27.7	26.0	30.1	28.9	28.6	25.4
9.0	31.0	30.2	29.8	25.6	29.1	25.7	27.4	25.7	28.1	27.9	26.9	25.1
9.5	30.4	31.8	31.1	26.9	29.9	28.7	27.4	26.7	30.1	29.7	29.5	27.1
10.0	30.8	32.1	31.8	26.1	29.3	29.7	29.4	25.0	29.0	27.6	26.5	25.1
10.5	31.2	30.8	30.1	29.1	31.0	30.2	30.1	26.4	30.5	30.1	30.0	26.8
11.0	32.0	32.4	31.9	32.0	33.2	32.4	33.0	29.6	31.9	29.7	29.0	28.7
11.5	34.5	33.9	32.8	32.9	36.1	34.0	32.7	33.2	34.9	32.1	32.0	31.9
12.0	35.1	35.4	34.2	31.5	36.4	35.1	34.4	31.5	36.1	33.2	32.1	29.8
12.5	33.6	33.7	33.3	28.7	32.9	29.9	33.2	28.4	31.1	27.0	26.4	26.0
Mean (x-axis)	31.8	31.6	31.1	27.9	31.4	30.3	29.9	26.9	31.3	30.3	29.8	26.8
σ_x	2.0	2.2	1.9	2.3	2.3	2.5	2.2	2.5	2.1	1.9	2.4	2.0
Mean (y-axis)	30.6				29.6				29.5			
σ_x	2.6				2.9				2.7			
λ (%)	46.2				65.4				73.1			

In the table : σ, standard deviation; λ, percentage of data in each layer that show a definite decrease trend in temperature towards the chamber sides

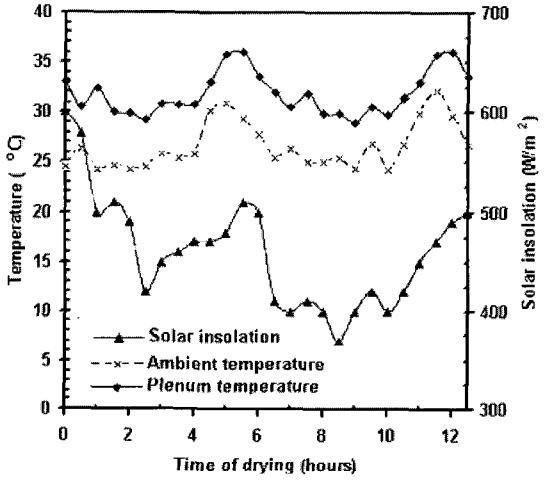

Fig. 4. Variation of solar insolation, and ambient and plenum chamber temperatures with drying time.

loss by the drying air (Brooker *et al.*, 1992). Since the top grain layer is exposed to convectional heat losses, this contributed to further lowering of the nodal temperature for the top layer.

The results of the comparison between the actual and predicted nodal temperatures are presented in Table 3. The table shows the computed residual error and prediction performance values, and the corresponding means and standard deviations (σ) of the residual errors. The residual errors were computed as shown in equation (8) while the prediction performance, which was based on a ±5.0% residual error interval, was calculated as in equation (9). The closer the residual errors are to zero, the more accurate the prediction levels are. In addition, the closer the standard deviation is to zero, the higher the precision (Kanali *et al.*,

Table 3 Residual errors (%) for grain temperature during solar drying

Drying time	Bottom layer				Middle layer				Top layer			
	Node number											
(Hours)	1	2	3	4	5	6	7	8	9	10	11	12
0.0	0.2	5.5	4.7	3.8	0.9	0.6	4.9	1.5	4.1	1.2	0.9	0.7
0.5	0.6	0.1	6.7	0.2	7.1	11.1	1.5	5.7	0.5	1.7	1.2	1.9
1.0	3.2	4.0	5.0	7.5	1.2	5.1	1.4	0.0	3.5	0.7	3.7	1.2
1.5	0.3	0.4	3.7	1.3	1.0	1.2	0.8	0.0	2.8	10.2	0.9	0.4
2.0	1.5	0.8	3.3	0.0	0.1	1.8	1.4	2.5	1.0	3.3	3.2	2.5
2.5	2.8	0.1	3.8	2.1	0.5	2.6	4.0	1.5	0.0	0.3	2.7	3.4
3.0	6.0	0.4	2.1	0.3	1.5	2.8	6.7	1.4	1.4	0.6	0.6	2.9
3.5	0.7	0.4	4.0	0.3	0.4	0.9	2.5	2.8	2.7	1.5	0.4	0.3
4.0	1.4	3.7	0.1	0.4	1.9	9.7	7.9	0.7	9.8	7.4	8.1	0.2
4.5	0.2	3.2	8.1	2.6	1.1	9.8	9.1	2.4	5.6	8.7	10.3	5.5
5.0	0.6	1.1	5.2	0.7	0.2	3.2	1.8	4.6	8.7	2.6	2.3	3.0
5.5	1.1	0.4	3.5	1.1	0.5	4.9	2.6	4.7	3.8	6.4	4.4	2.0
6.0	0.5	4.6	8.2	0.0	0.2	6.5	6.4	4.1	1.5	1.3	1.2	0.7
6.5	0.7	0.3	15.1	2.7	0.1	2.5	9.1	3.5	11.8	6.8	1.9	0.7
7.0	1.1	0.1	8.7	0.2	0.3	7.5	5.5	4.8	0.2	0.3	8.1	1.4
7.5	1.2	0.8	1.7	0.8	3.5	2.9	0.2	1.9	2.6	2.5	0.1	1.1
8.0	3.3	0.1	5.6	0.1	0.8	6.7	2.4	7.4	2.5	2.3	2.4	5.4
8.5	2.9	0.6	0.9	0.2	0.1	8.7	3.8	1.3	2.2	0.4	4.7	0.6
9.0	0.8	0.9	4.6	2.5	1.9	10.7	1.6	4.1	7.0	4.7	4.3	0.0
9.5	0.5	0.5	1.9	0.6	0.9	4.8	8.0	1.5	0.1	4.6	3.2	3.5
10.0	0.1	0.3	7.7	2.9	0.1	1.9	3.4	1.6	3.9	7.9	8.1	1.5
10.5	1.0	1.5	3.1	0.3	0.2	2.5	0.7	2.5	0.4	1.6	3.0	3.7
11.0	2.3	1.5	6.2	0.2	1.2	1.0	2.2	1.6	3.1	1.7	2.7	4.0
11.5	1.0	0.3	1.1	0.2	1.8	4.0	6.6	2.7	3.4	5.1	8.0	0.5
12.0	2.6	0.1	3.5	0.0	2.5	0.7	0.2	4.6	2.2	1.1	3.6	0.5
12.5	1.6	0.4	9.1	0.7	0.2	9.6	4.1	4.6	0.7	1.2	1.3	0.8
Mean	1.5	1.2	4.9	1.2	1.2	4.8	3.8	2.9	3.3	3.3	3.5	1.9
σ	1.3	1.6	3.3	1.7	1.5	3.4	2.8	1.8	3.1	2.9	2.8	1.6
η_x(%)	96.2	96.2	61.5	96.2	96.2	61.5	73.1	92.3	80.8	73.1	80.8	92.3
R^2	0.990	0.982	0.943	0.941	0.980	0.943	0.981	0.972	0.940	0.991	0.982	0.981
η_y(%)			87.5				79.8		81.7			
$\eta_{overall}$(%)							83.3					

In the table : σ, standard deviation; η_x, η_y and $\eta_{overall}$, lateral, vertical and overall prediction performance

2000).

The finite element model attained a high prediction performance level for temperature distribution since 83.3% of the total data had residual errors within the ±5% interval. In addition, the low residual error mean (1.2–4.9%) and standard deviation (1.3–3.4%) indicate that the model achieved accurate and precise prediction levels for temperature. The performance levels in the lateral direction (x-axis) ranged from a modest 61.5–96.2% for Nodes 1-4 and Nodes 5–8, and from 73.1–92.3% for Nodes 9-12, indicating satisfactory lateral temperature distribution prediction. Similarly, satisfactory prediction performance levels (lying between 79.8 and 87.5%) were realized in the vertical direction (y-axis). This implies that the finite element model achieved satisfactory 2-D temperature distribution prediction for the solar grain dryer.

The linear regression analysis results relating the predicted and measured nodal temperature data are also presented in Table 3. The high coefficients of determination (R^2) ranging from 0.940–0.991 that were obtained indicate that there was a high correlation between the predicted and measured nodal temperatures. This further confirms that the finite element model achieved satisfactory performance in the prediction of temperature distribution during solar

drying of the rice.

Conclusions

The results of this study show that the finite element model achieved an overall prediction performance level of 83.3.0% based on a ±5% residual error interval for grain temperature distribution in the solar dryer. Satisfactory prediction levels were also realized for the lateral (61.5–96.2%) and vertical (73.1–92.3%) directions of grain drying. These results indicate that it is feasible to use a 2-D finite element model to predict temperature distribution in a solar grain dryer. The method therefore offers significant advantages over existing conventional methods, as it provides relatively accurate predictions of temperature distribution. It also offers considerable advantage over experimental determination of temperature as it reduces time requirements and the need for expensive measuring equipment.

References

ASAE standards. Standards engineering practices data. American Society of Agricultural Engineers, St Joseph, Michigan, USA (1997).

Baker, A. J., D. W. Pepper. Finite elements 1-2-3. McGraw-Hill, International edition, New York (1991).

Basunia M. A., B. K. Bala., T. Abe. Application of finite element method for the simulation of temperature distribution during storage of rough rice in cylindrical bin. Journal of Agricultural Mechanization in Asia, Africa and Latin America, 27(2):33-40 (1996).

Bonazzi C., F. Courtois, C. Geneste,, B. Pons,, M. C. Lahon, J. J. Bimbenet. Experimental study on the quality of rough rice related to drying conditions. In Drying, pp. 1031-1036 (1994).

Brooker, D.B., F. W. Bakker-Arkema, C. W. Hall. Drying and storage of grains and oilseeds. Van Nostrand Reinhold, New York (1992).

Holman, J.P.: Heat transfer, McGraw Hill, Singapore (1992).

Jia, C., C. W. Cao.: Mathematical simulation and experimental research of temperature pattern in wheat storage bin. Transactions of the Chinese Society of Agricultural Machinery, 29(1):70-74 (1998).

Jia, C., D. W. Sun, C. W. Cao. Finite element prediction of transient temperature distribution in a grain storage bin. Journal of Agricultural Engineering Research, 76: 323-330 (2000).

Kanali, C. L., C. Nindo, J. Mailutha, A. Anyangu, J. Nozaka,, H. Murase. Neural network prediction of grain moisture content in a deep bed dryer. Applied Biological Science, 6:87-100 (2000).

Kristoferson, L. A., V. Bokalders. Renewable energy technologies: their applications in developing countries. Intermediate Technologies Publications, London (1991).

Nindo, C. I. Studies in the sundrying of raw rough rice. PhD thesis, Iwate University, Japan (1995).

Oothuizen, P. H. A numerical model of a natural convection solar grain dryer: development and validation. In Solar Drying in Africa. *Proceedings of a workshop held in* Dakar, Senegal. 21-24 July 1986. IDRC, Ottawa, Canada, pp. 234-252 (1987).

Saleh T., M. A. Sarker. Performance of a PV operated forced convection solar energy dryer. Bangladesh University of Engineering and Technology, Bangladesh (2002).

Segerlind L. J.: Applied finite element analysis. John Wiley and Sons, New York, (1984).

Suroso, A. Tani, Y. Nishiura, H. Murase, N. Honami, and H. Takigawa.: Finite element analysis for temperature distribution in interior of plant culture vessel. Agricultural Mechanization in Asia, Africa and Latin America, 26(3):19-23 (1995).